WEP Warwick Evans Publishing

International Journal of Natural Resources and Environmental Studies

ISSN: 3006-2012 (Print), ISSN: 3006-0834 (Online) | Volume 8, Number 3, Year 2026
DOI: https://doi.org/10.62051/ijnres.v8n3.12
Journal homepage: https://wepub.org/index.php/IJNRES/index

Spatiotemporal Dynamics of Carbon Emissions and the Role of Land-Use Change: A County-Level Analysis in Ganzhou, China

Sichen Xi

College of Architecture and Art, Central South University, Changsha, China

ABSTRACT

Ganzhou has experienced rapid land-use and socioeconomic transformation over the past two decades, yet county-level analyses of carbon emission dynamics and their land-use drivers remain limited. This study examines the spatiotemporal evolution of county-level CO_2 emissions in Ganzhou from 2000 to 2020 using emission data from the China Emission Accounts and Datasets, land-use maps, and socioeconomic statistics. Spatial analytical methods, including Moran's I and the standard deviational ellipse, together with landscape metrics and correlation analysis, were applied to explore emission patterns and their relationship with land-use structure. Results show that total CO_2 emissions increased from 9.59 Mt in 2000 to 36.36 Mt in 2020, although the growth rate slowed after 2010. The spatial pattern shifted from a "central high–peripheral low" structure to a more dispersed pattern characterized by "central > northeast > south > west." Built-up land expansion and greater patch aggregation are significantly positively correlated with emissions, whereas larger and more connected forest patches show significant negative correlations. These findings highlight the importance of controlling urban expansion, improving forest connectivity, and promoting coordinated regional mitigation strategies to support carbon reduction and sink enhancement.

KEYWORDS

Land Use; CO2 Emissions; Spatial Autocorrelation; Landscape Metrics.

1. INTRODUCTION

1.1. Research Background

At the 75th session of the United Nations General Assembly, Xi Jinping announced that China aims to achieve carbon peaking by 2030 and carbon neutrality before 2060. Since the Industrial Revolution, rapid economic and industrial expansion has intensified environmental pressures, with issues such as the greenhouse effect increasingly constraining sustainable urban development. Previous studies suggest that land-use change has become the second-largest source of greenhouse gas emissions after fossil fuel combustion, as processes such as urban expansion and deforestation alter regional carbon sources and sinks and reshape emission patterns. However, most existing research focuses on provincial or prefectural scales and economically developed regions, while county-level analyses in less-developed areas remain limited. Downscaling analysis to the county level can better capture spatial heterogeneity and local emission dynamics, thereby providing more targeted policy support for achieving the "dual-carbon" goals and promoting low-carbon regional development.

1.2. Literature Review

Current research on carbon emissions can be broadly categorized into four main areas: carbon emission accounting methods, spatiotemporal evolution characteristics, influencing factors, and urban carbon reduction technologies [1].

1.2.1. Review of Carbon Emission Accounting Methods

1.2.1.1. Studies Based on the Emission Factor Method

The emission factor method is fundamentally based on carbon emission inventories (**Table 1**). For each emission source, corresponding activity data (AD) and emission factors (EF) are identified. The carbon emissions from a specific source are then estimated as the product of activity data and the associated emission factor [2]. In 2017, Ouyang Xiaoling and Lin Boqiang [3] applied the emission factor method to estimate direct carbon emissions generated by urban activities, including industrial energy consumption and transportation energy use. In 2022, Wang Zhiqiang et al. [4] constructed an urbanization accounting framework from three dimensions—population, industry, and land—and calculated China's urbanization-related carbon emissions from 2002 to 2017 based on the emission factor method. These studies demonstrate the adaptability of the emission factor approach across different thematic and sectoral contexts, particularly in urban-scale carbon emission assessments.

Table 1. Urban carbon emission accounting indicator system

Carbon Source	Primary Indicator	Secondary Indicator	Required Data
Residential source	Population urbanization carbon emissions	Direct carbon emissions Indirect carbon emissions	Consumption of urban residents Consumption expenditure of urban residents
Production source	Industrial urbanization carbon emissions	Production energy consumption Industrial production processes	Energy consumption of the secondary and tertiary industries Output of steel, cement, and other industrial products
Carbon loss source	Land urbanization carbon emissions	Occupation of construction land	Area of cultivated land, forest land, grassland, etc., occupied by construction land

1.2.1.2. Studies Based on the Mass Balance Method

The mass balance method is based on the law of conservation of mass and estimates carbon emissions by subtracting non-CO_2 carbon outputs from total carbon inputs within a production process. This approach is mainly applied to sector-specific emission accounting where detailed material flow data are available. For example, Hampf et al. (2019) developed a stochastic mass balance framework incorporating physical production constraints to estimate CO_2 emission factors for fossil-fuel power plants in the United States [5].

1.2.1.3. Direct Measurement Method

The direct measurement method calculates total emissions using on-site monitoring and continuous measurement systems. While it provides relatively high accuracy at facility or micro scales, its high cost and limited data availability restrict its application in large-scale regional or city-level carbon accounting.

1.2.1.4. Remote Sensing-Based Estimation

Remote sensing methods estimate emissions by integrating satellite observations with statistical data. Nighttime light data are widely used as a proxy for economic activity and energy consumption. For instance, Niu Yawen et al. used NPP–VIIRS nighttime light data to estimate county-level land-use carbon emissions in the Chang–Zhu–Tan region [6], while Yu Bo et al. applied the same dataset to

estimate monthly emissions in the Harbin–Changchun urban agglomeration [7]. However, estimates based solely on nighttime light data may be affected by observational errors, atmospheric interference, and sensor saturation, requiring supplementary statistical calibration.

1.2.2. Review of Spatiotemporal Evolution Characteristics

The spatiotemporal evolution of carbon emissions is commonly analyzed using tools such as the coefficient of variation, exploratory spatial data analysis (ESDA), and spatial autocorrelation. For example, Yoichi Kaya introduced the Kaya identity to decompose CO2drivers [8], and recent work has applied extended STIRPAT models with spatiotemporal GWR to probe urbanization-driven heterogeneity (e.g., Zhang et al. [9]). Two gaps remain: most studies operate at provincial or prefectural scales, limiting insight into intra-county heterogeneity, and few systematically combine landscape-configuration metrics with spatiotemporal analyses of emissions. To address these gaps, this study integrates standard deviational ellipse (SDE) and Moran's I analyses with landscape metrics computed by FRAGSTATS and Pearson correlation testing to assess land-use–emission coupling at the county scale in Ganzhou.

2. STUDY AREA AND DATE SOURCES

2.1. Study Area

Ganzhou is located in southern Jiangxi Province, China, bordering Ji'an and Fuzhou to the north, Sanming and Longyan (Fujian Province) to the east, and Meizhou and Heyuan (Guangdong Province) to the south. The municipality covers approximately 39,363 km², making it the largest prefecture-level city in Jiangxi in terms of land area. Ganzhou is an important resource-based city and serves as a sub-central city of Jiangxi Province. As a less-developed city undergoing rapid industrialization and urbanization, industrial energy consumption has become the dominant source of carbon emissions. In 2012, Ganzhou was selected as a national low-carbon pilot city, making it a representative case for examining carbon emission dynamics and low-carbon transition in resource-dependent regions.

2.2. Data Sources

2.2.1. Land Use Data

Land use data were obtained from the Resource and Environmental Science Data Center of the Chinese Academy of Sciences. Raster land use datasets for the years 2000, 2005, 2010, 2015, and 2020 were employed in this study.

2.2.2. Socioeconomic Data

Socioeconomic data were primarily collected from publicly available statistical yearbooks published on the official website of the Ganzhou Municipal People's Government and supplemented through consultation with the Ganzhou Municipal Bureau of Statistics.

2.2.3. Carbon Emission Data

Carbon emission data for Ganzhou were obtained from the county-level CO2 emission dataset released by the China Emission Accounts and Datasets (CEADs). The CEADs dataset estimates CO2emissions for 2,735 counties across China by integrating DMSP/OLS nighttime lights program and NPP/VIIRS nighttime lights program data through a particle swarm optimization–back propagation (PSO–BP) algorithm[10]. By harmonizing multi-source nighttime light imagery and applying scale normalization, the dataset achieves high consistency with energy-based carbon accounting results.

2.3. Research Methods

2.3.1. Spatial Autocorrelation Indicators

This study uses Moran's I to examine the spatial autocorrelation of carbon emissions. Global Moran's I evaluates the overall spatial dependence of emissions across the study area, with values ranging from −1 to 1; positive values indicate spatial clustering, while negative values indicate dispersion.

2.3.2. Standard Deviational Ellipse

The Standard Deviational Ellipse (SDE) method is applied to analyze the spatial distribution and evolution of carbon emissions. Key parameters include the mean center, major and minor axis lengths, ellipse area, and azimuth angle. The mean center indicates the spatial centroid of emissions, while the axis lengths and ellipse area reflect the degree of spatial dispersion. The azimuth angle reveals the dominant directional trend of emission distribution, allowing the spatiotemporal evolution of carbon emissions in Ganzhou to be effectively characterized.

2.3.3. Landscape Pattern Indices

Landscape pattern indices integrate both landscape structure and quantitative landscape metrics. Calculating landscape indices for a given region helps to evaluate its current landscape configuration and land-use structure. Comparing indices across different time periods enables the identification of landscape pattern changes and land-use transformation trends, as well as the analysis of underlying driving mechanisms. In this study, landscape pattern indices were calculated using FRAGSTATS, developed by Oregon State University. The selected indices are presented in **Table 2**.

Table 2. Landscape pattern indicators

No.	Indicator Name	Description
1	Patch Area (AREA)	Total area of a patch
2	Class Area (CA)	Total area of patches belonging to a specific landscape class
3	Largest Patch Index (LPI)	Used to identify the dominant patch type within the landscape
4	Number of Patches (NP)	Total number of patches, or the number of patches of a specific landscape class
5	Patch Density (PD)	Reflects the density of a particular patch type in the landscape. It can indicate the overall heterogeneity and fragmentation of the landscape, as well as the fragmentation degree of a specific type, showing heterogeneity per unit area
6	Shape Index (SHAPE)	Measures the complexity of a patch's shape by calculating its deviation from a circle or square of the same area
7	Fractal Dimension Index (FRAC)	Non-integer dimension of irregular geometric shapes in the landscape, reflecting the complexity of landscape form
8	Euclidean Nearest-Neighbor Distance (ENN)	Measures the absolute distance between two points in multidimensional space
9	Aggregation Index (AI)	Examines the connectivity between patches of each landscape type. A lower value indicates a more dispersed landscape
10	Patch Cohesion Index (COH)	Reflects the aggregation or dispersion state of patches within the landscape
11	Perimeter-Area Ratio (PARA_MN)	Ratio of patch perimeter to area
12	Landscape Fragmentation (LF)	Characterizes the degree to which the landscape is divided into fragments, reflecting the complexity of the spatial structure and, to some extent, the extent of human disturbance on the landscape

3. SPATIOTEMPORAL PATTERNS AND EVOLUTION OF CARBON EMISSIONS

3.1. Temporal Variation Characteristics of Carbon Emissions in Ganzhou

Carbon emission statistics for both municipal and county levels in Ganzhou are presented in **Figure 1**. From 2000 to 2020, total carbon emissions increased from 9.59 million tons to 36.36 million tons, representing nearly a fourfold rise over the two decades. At the county level, the spatial distribution of emissions shows significant heterogeneity. In 2020, Zhanggong recorded the highest emissions, reaching 7.08 million tons and accounting for approximately 19% of the municipal total. Ruijin ranked second with emissions of 4.71 million tons (about 12%). Together with Nankang and Ganxian, the three central municipal districts contributed about 31.8% of Ganzhou's total emissions.

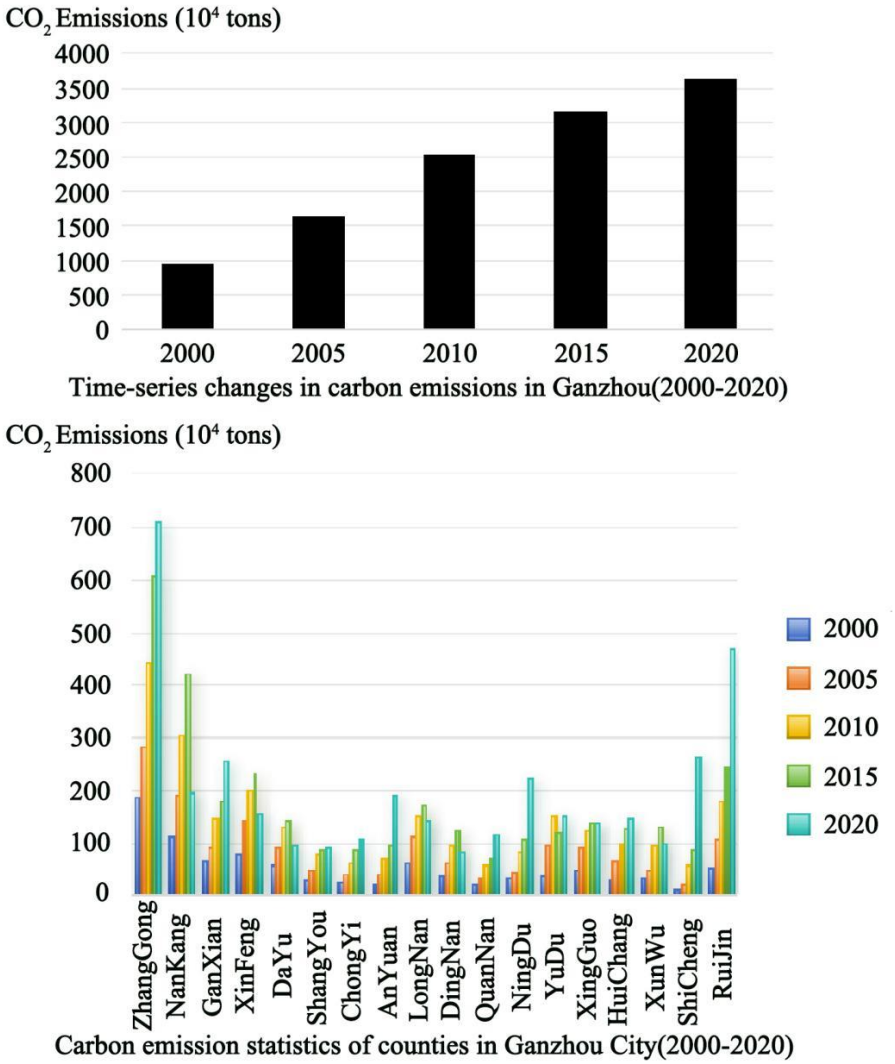

Figure 1. Total carbon emissions in Ganzhou City and time-series changes in counties

At the same time, this study calculated the slope value of carbon emissions for each county (district) over the period 2000–2020. A positive slope indicates a positive correlation between carbon emissions and time, suggesting an increasing trend, whereas a negative slope implies a declining trend over the study period. The magnitude of the slope represents the intensity of change: larger absolute values correspond to stronger growth or decline trends. The results are presented in **Table 3**.

Table 3. Carbon emission trends in various regions

Slope Value	2000-2010	2010-2020
Zhanggong	25.37	26.76
Nankang	19.33	-10.75
Ganxian	7.73	10.89
Xinfeng	12.25	-4.53
Dayu	7.49	-3.51
Shangyou	4.65	1.45
Chongyi	3.76	4.52
Anyuan	4.71	12.13
Longnan	8.72	-0.92
Dingnan	5.76	-1.26
Quannan	3.38	5.79
Ningdu	4.85	14.15
Yudu	11.36	0.00
Xinguo	7.35	1.39
Huichang	6.83	4.79
Xunwu	6.04	0.49
Shicheng	4.35	20.74
Ruijin	12.45	29.22

During the period from 2000 to 2010, carbon emissions in all counties and districts exhibited an upward trend. Among them, Zhanggong showed the most pronounced growth, with a slope value of 25.37, indicating the strongest increase in emissions over this decade. In contrast, Quannan demonstrated the weakest growth trend, with a slope value of 3.38, reflecting relatively moderate emission expansion. From 2010 to 2020, the overall growth rate of carbon emissions in Ganzhou began to decelerate. Nevertheless, Zhanggong, Ganxian, Ruijin City, and Shicheng continued to exhibit significant growth trends. Among these, Zhanggong again recorded the strongest increase, with a slope value of 26.75, indicating persistent emission pressure in the core urban area despite the broader slowdown across the municipality.

3.2. Spatial Variation Characteristics of Carbon Emissions in Ganzhou

At the municipal scale, carbon emissions in Ganzhou were relatively low in 2000, with a total of 9.59 million tons. The most pronounced increase occurred during the period from 2000 to 2010, when total emissions rose by approximately 15.64 million tons over the decade. Spatially, emissions exhibited a clear pattern characterized by “higher in the central area and lower in the periphery.” The main urban area centered on Zhanggong constituted the core high-emission zone, while the western, northeastern, and southeastern parts of the municipality formed relatively low-emission areas.

Between 2010 and 2020, although the growth rate of carbon emissions slowed compared with the previous decade, the total increase during this period still reached approximately 11.13 million tons. Moreover, some counties maintained higher average annual growth rates relative to the 2000–2010 period. By 2020, the spatial pattern of carbon emissions evolved into a structure described as “central > northeastern > southern > western,” forming a contiguous high-emission belt centered on Zhanggong and Ruijin.

3.2.1. Spatial variation trend of county-level carbon emissions

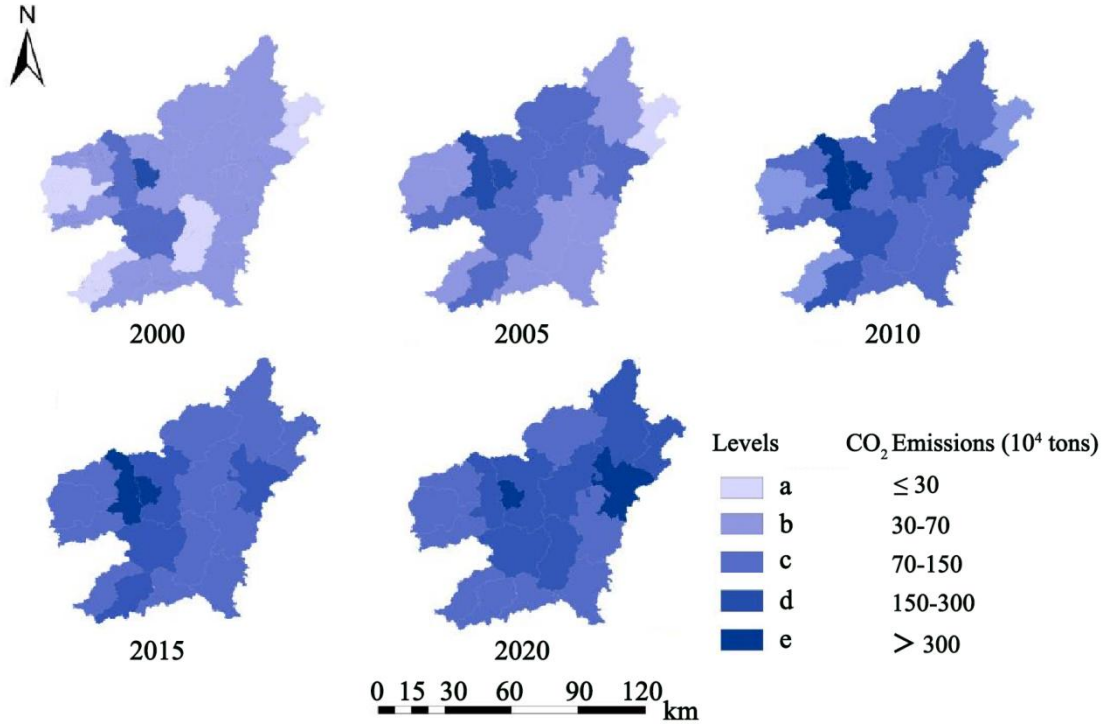

Figure 2. Spatiotemporal evolution of county-level carbon emissions from 2000 to 2020

For analytical clarity, county-level carbon emissions were classified into five categories: (a) Low emission zone (≤0.3 million tons per year); (b) Moderate emission zone (0.3–0.7 million tons per year); (c) Medium emission zone (0.7–1.5 million tons per year); (d) High emission zone (1.5–3.0 million tons per year); (e) Very high emission zone (≥3.0 million tons per year).

From a temporal perspective, in 2000 only Zhanggong reached the high-emission category (1.875 million tons), while Nankang and Xinfeng were classified as medium-emission areas. Most other counties fell into the moderate category. Between 2000 and 2015, Zhanggong remained the dominant emission center, and by 2010 both Zhanggong and Nankang had entered the very high emission category, widening the gap with other counties. By 2020, the very high emission group consisted of Zhanggong (7.088 million tons) and Ruijin (4.72 million tons), while Nankang shifted to the high-emission category (1.959 million tons). Overall, most counties had reached at least the medium-emission level by 2020. Based on this classification scheme and the spatial distribution of county-level emissions (**Figure 2**), substantial spatial heterogeneity is observed at the county scale.

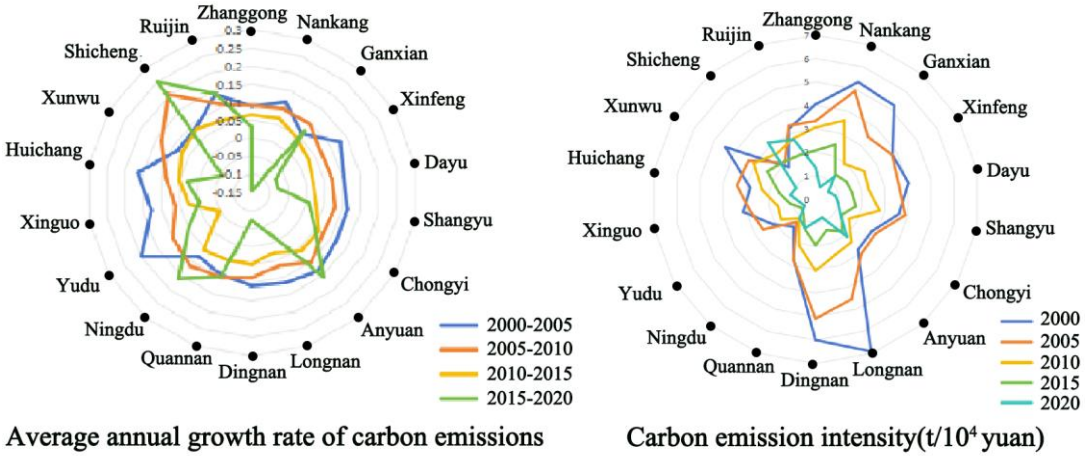

Figure 3. Average annual growth rate and intensity of carbon emissions from 2000 to 2020

Table 2 shows that carbon emissions grew rapidly across nearly all counties during 2000–2010, with many units recording double-digit average annual increases (Yudu and Shicheng among the highest). After 2010, growth rates and emission intensity generally declined: 2010–2015 saw no county exceed a 10% annual rate, and 2015–2020 included seven counties with negative growth (e.g., a −14% decline in Nankang). Based on growth trajectories and baselines, the 18 county/district units cluster into three types. First, frontier or underdeveloped areas (e.g., Anyuan, Shicheng, Dingnan) have low initial emissions but high recent growth driven by accelerating energy use as industrialization begins. Second, mineral-resource regions (e.g., Ningdu, Xingguo, Xinfeng) started from high baselines and have moderated growth since ~2010 due to technological improvements and stricter environmental controls. Third, mature urban districts (e.g., Zhanggong, Ganxian District, Ruijin) sustain large emission bases with slower growth, making them priority targets for mitigation despite falling intensity. Overall, the post-2010 slowdown and emerging negative trends in several counties suggest that structural change and policy interventions are beginning to curb emission growth, though spatial heterogeneity remains pronounced.

3.2.2. Spatial Migration Characteristics of Carbon Emissions

To further examine the spatial evolution of carbon emissions in Ganzhou, this study applied the Standard Deviational Ellipse (SDE) method in ArcGIS 10.6 to analyze the spatial migration characteristics from 2000 to 2020(**Figure 4**).

The results show that the spatial pattern of carbon emissions remained relatively stable from 2000 to 2015, with only slight changes in the lengths of the major and minor axes. The ellipse consistently covered high-emission areas such as Zhanggong, Ganxian, Nankang, Yudu, and Xinfeng, while showing a gradual expansion toward the northeast, indicating a slight shift of emission growth in that direction. From 2015 to 2020, the northeastward expansion became more pronounced. The major axis extended toward Ruijin City, reflecting its rapid increase in carbon emissions, which reached 4.72 million tons in 2020 and ranked second in the municipality. Despite these directional adjustments and increasing concentration, the centroid of the ellipse showed little movement over the study period. This stability mainly reflects the dominant role of Zhanggong, the central urban area of Ganzhou, whose strong population, economic scale, and industrial base have long anchored the spatial center of carbon emissions in the municipality.

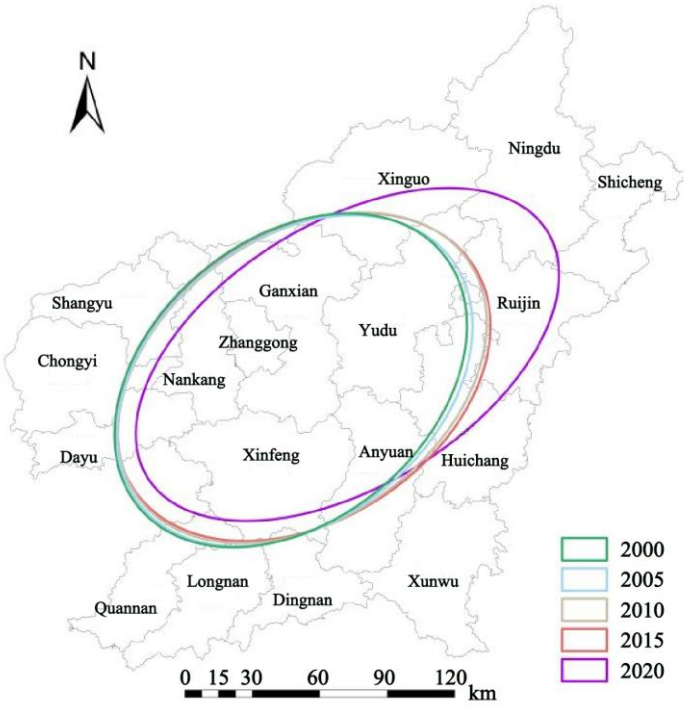

Figure 4. Spatiotemporal trends of carbon emissions

3.2.3. Global Spatial Autocorrelation Analysis of Carbon Emissions

Using ArcGIS 10.6, carbon emission data from the 18 counties and districts were analyzed, and the corresponding Moran's I values, Z-scores, and P-values were calculated (**Table 4**).

Table 4. Carbon emission potential based on Moran's I index (2000-2020)

years	Moran's I	Z Value	P
2000	0.416	2.729	0.0063
2005	0.259	1.70	0.089
2010	0.314	2.03	0.042
2015	0.362	2.36	0.018
2020	0.102	0.93	0.356

The results indicate that only in 2000 did Moran's I exceed 0.4, with a Z-score greater than 2.5 and a P-value less than 0.01. This demonstrates that carbon emissions in 2000 exhibited highly significant positive spatial autocorrelation, meaning that counties with high (or low) emission levels were spatially adjacent to one another. In other words, the carbon emission pattern in 2000 displayed a pronounced spatial clustering effect, characterized by a clear aggregation of high-emission and low-emission areas.

However, the spatial clustering effect gradually weakened to varying degrees. By 2020, the spatial autocorrelation reached its lowest level, with Moran's I decreasing to 0.102. This suggests a marked tendency toward spatial dispersion. The weakening of spatial dependence not only confirms that the carbon emission pattern in 2020 no longer exhibits a distinctly monocentric structure, but also reflects increasing interregional heterogeneity in emission levels.

4. ANALYSIS OF LAND USE INFLUENCING FACTORS

4.1. Overall Analysis of Land Use Changes

The land use data used in this study were obtained from the Resource and Environment Science and Data Center. Land use types for the municipal area of Ganzhou in 2000, 2005, 2010, 2015, and 2020 were compiled and summarized (**Table 5**). The dataset includes six major categories: Cropland Area (CA), Forestland Area (FA), Grassland Area (GA), Water Area (WA), Construction Land Area (CLA), and Bare Land Area (BLA). Their spatial distribution is illustrated in **Figure 5**.

Table 5. Ganzhou Land Use Data (2000-2020)

Unit (hectares)	2000	2005	2010	2015	2020
CA	453441	695563	694727	687992	681436
FA	2955897	2945990	2901795	2938351	2915379
GA	224653	218588.8	217063	216043	230156.1
WA	37979	38094	38282.2	38189	38259
CL A	36713	38019	45918	55526	70968
BLA	194388	129124	55449	30047	28047

Further analysis of land-use change in Ganzhou from 2000 to 2020 reveals substantial differences among land-use categories(**Table 6**). Built-up land experienced the most dramatic expansion, increasing from 36,713 ha to 709,658 ha, largely driven by rapid urbanization, outward urban expansion, and the economic transition toward secondary and tertiary industries. The largest increases occurred in Zhanggong and Nankang, contributing to higher energy consumption and widening carbon emission gaps with other counties.

Cultivated land showed a phased trend. Although total area increased overall, it has gradually declined since 2005, with a net loss of about 6,556 ha between 2015 and 2020. Cropland is mainly

distributed in valley plains such as Xinfeng and Ruijin, where labor transfer to secondary and tertiary industries has accelerated urbanization and indirectly increased energy consumption and emissions.

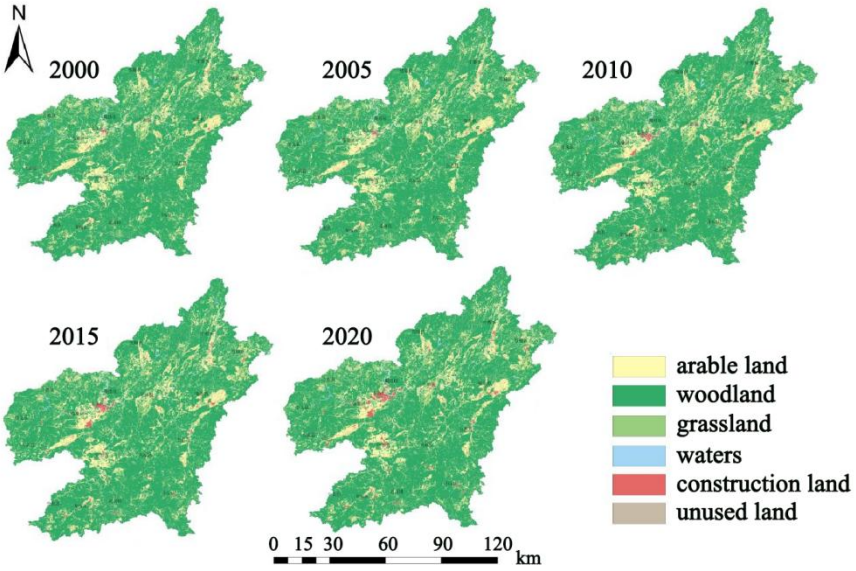

Figure 5. Land use distribution in Ganzhou (2000-2020)

Forest land remains the dominant land-use type, accounting for over 70% of the total area, with a forest coverage rate of 76.23% in 2020. However, forest area declined slightly from 2.96 million ha in 2000 to 2.92 million ha in 2020, weakening the region's natural carbon sink capacity. In contrast, grassland and water bodies showed relatively stable changes, indicating limited but improvable carbon sink potential.

Table 6. Average annual change and rate of land use types at different times

Categories/Year	2000-2010		2010-2020		2000-2020	
	Annual Change (ha)	Change Rate (%)	Annual Change (ha)	Change Rate (%)	Annual Change (ha)	Change Rate (%)
CA	241286.00	4.36	-13290.90	-0.19	227995.10	2.06
FA	-54102.30	-0.18	13584.70	0.05	-40517.60	-0.07
GA	-7589.30	-0.34	13092.40	0.59	5503.10	0.12
WA	302.60	0.08	-22.50	-0.01	280.10	0.04
CLA	9205.00	2.26	25050.40	4.45	34255.40	3.35
BLA	-138939.00	-11.7	-27402.00	-6.59	-166341.00	-9.23

4.2. Analysis of Land-Use Influencing Factors

The statistical software SPSS was applied to examine the relationships between the calculated landscape pattern indices and carbon emissions in Ganzhou, thereby identifying the potential influence of land-use spatial structure on regional carbon emissions. The calculated results of the landscape pattern indices are presented in **Table 7**.

Table 7. Landscape Pattern Index of Ganzhou, 2000-2020

	2000					
	CA	FA	GA	WA	CLA	BLA
AREA	66.3283	858.0122	58.2723	107.9869	13.6282	3.33
CA	114350.0	363797.1	38168.3	10366.74	5587.56	6.66
LPI	5.5617	16.823	0.3498	1.7454	0.1975	0.0007

NP	1724	424	655	96	410	2
PD	0.3239	0.0797	0.1231	0.018	0.077	0.0004
SHAPE	2.1364	2.0481	2.013	1.8935	1.3842	1.2436
FRAC	1.1116	1.0882	1.1028	1.0882	1.058	1.0469
ENN	206.1946	159.2828	496.515	1788.948	719.4536	22980.0196
AI	92.0622	97.2904	92.2713	92.8095	90.2951	90
COH	99.263	99.9044	97.712	99.6467	94.8255	83.5593
PARA_MN	335.7024	240.0637	199.260	312.5516	245.066	281.8627
LF	0.9966	0.9131	0.9999	0.9997	1	1

2005

	CA	FA	GA	WA	CLA	BLA
AREA	86.2091	882.9486	58.4639	128.1767	14.4902	3.285
CA	116123.6	362891.8	37066.1	10382.31	5854.05	6.57
LPI	5.5779	15.4395	0.3492	1.7561	0.1972	0.0007
NP	1347	411	634	81	404	2
PD	0.253	0.0772	0.1191	0.0152	0.0759	0.0004
SHAP)	2.433	2.2145	2.0969	2.0383	1.4179	1.2436
FRAC	1.1289	1.0959	1.1085	1.0974	1.061	1.0484
ENN	245.5308	157.478	524.327	2244.166	733.4675	22997.6173
AI	91.8862	97.1815	91.9642	92.6599	90.2631	89.8438
COH	99.3279	99.8783	97.6434	99.6527	94.9429	83.4374
PARA_MN	274.0352	221.2417	184.318	261.0598	235.3378	286.6162
LF	0.9964	0.9338	1	0.9997	1	1

2010

	CA	FA	GA	WA	CLA	BLA
AREA	80.3435	865.561	59.7933	124.53	30.1576	3.195
CA	112561.2	359207.8	38267.7	10460.52	11821.77	6.39
LPI	5.3316	14.974	0.3488	1.7706	0.5965	0.0007
NP	1401	415	640	84	392	2
PD	0.2632	0.078	0.1202	1.7706	0.0736	0.0007
SHAPE	2.3718	2.2143	2.0613	2.0062	1.3942	1.2436
FRAC	1.1255	1.0965	1.106	1.0955	1.0587	1.0512
ENN	243.5397	172.2212	532.135	2081.381	752.5741	22997.6173
AI	91.8321	97.2128	92.2293	92.7623	94.4977	88.8
COH	99.286	99.8729	97.6738	99.6542	98.113	83.2033
PARA_MN	275.6789	203.6117	184.946	267.7466	239.8845	294.8718
LF	0.9968	0.9363	1	0.9997	0.9999	1

2015

	CA	FA	GA	WA	CLA	BLA
AREA	66.1384	788.6412	56.6019	109.926	36.9876	3.375
CA	110186.5	357254.4	37866.6	10442.97	16533.45	6.75
LPI	5.1061	16.3217	0.3489	1.7444	0.843	0.0007
NP	1666	453	669	95	447	2
PD	0.313	0.0851	0.1257	0.0178	0.084	0.0004
SHAPE	2.1549	2.0421	1.9864	1.8858	1.382	1.2436
FRAC	1.1128	1.0897	1.1015	1.0868	1.057	1.0454
ENN	214.2046	170.8805	496.933	1847.458	722.6824	22997.6173
AI	91.9024	97.2726	92.3258	92.8794	95.2602	90.1515
COH	99.2301	99.8934	97.6478	99.645	98.3315	83.6778
PARA_MN	323.7251	248.1794	203.105	308.0457	234.4613	277.381
LF	0.9971	0.9244	1	0.9997	0.9999	1

	2020					
	CA	FA	GA	WA	CLA	BLA
AREA	74.7937	746.4617	57.4101	125.5945	51.383	3.555
CA	106880.1	352329.9	39612.9	10424.34	23070.96	7.11
LPI	4.1902	14.3301	0.3493	1.5471	1.0837	0.0007
NP	1429	472	690	83	449	2
PD	0.2684	0.0887	0.1296	0.0156	0.0843	0.0004
SHAPE	2.3524	2.1394	2.0093	2.1104	1.4272	1.2381
FRAC	1.1244	1.0956	1.1023	1.0999	1.0602	1.0468
ENN	249.8456	176.6079	494.691	2216.739	718.5489	22981.0378
AI	91.5191	97.1783	92.3223	92.7601	95.7352	90
COH	99.1755	99.8702	97.6062	99.5802	98.6491	84.0975
PARA_MN	277.6284	216.8477	197.374	257.5098	220.2369	273.5931
LF	0.9979	0.9389	1	0.9998	0.9998	1

Built-up land serves as the primary carrier of human activities and is also the main source of carbon emissions. Therefore, this study first examines the relationship between the landscape pattern indices of built-up land and carbon emissions. Based on SPSS 26, a bivariate correlation analysis was conducted to investigate the relationship between the landscape pattern indices of built-up land and carbon emissions in Ganzhou. The results of the correlation analysis are presented in **Table 8** and **Table 9.**

Table 8. Pearson correlation analysis between construction land use and carbon emissions

		CA	LPI	PD	SHAPE	ENN	AI	COH
Emissions(10^4tons)	correlation	.958*	.973**	0.699	0.315	-0.072	.953*	.942*
	Sig.	0.01	0.005	0.189	0.605	0.908	0.012	0.017
	number	5	5	5	5	5	5	5

The results indicate that LPI of built-up land shows a significant positive correlation with carbon emissions. This is followed by CA, AI, and COH, which also exhibit positive correlations with carbon emissions. In contrast, ENN is negatively correlated with carbon emissions. These findings suggest that the area of built-up land is significantly positively correlated with carbon emissions. According to the land-use analysis presented earlier, the built-up land area in Ganzhou increased substantially from 2000 to 2020, which is consistent with the overall upward trend in carbon emissions during the same period. Furthermore, the correlation analysis indicates that both the connectivity and aggregation degree of built-up land are positively associated with carbon emissions. Therefore, stronger clustering and internal aggregation effects of built-up land tend to lead to increased carbon emissions.

Table 9. Pearson correlation analysis of forest land and carbon emissions

		CA	LPI	PD	SHAPE	ENN	AI	COH
Emissions (10^4tons)	correlation	-.959**	-0.62	0.789	0.02	.919*	-0.367	-0.567
	Sig.	0.01	0.264	0.113	0.974	0.027	0.544	0.319
	number	5	5	5	5	5	5	5

Forest land accounts for more than 70% of the total land area of Ganzhou. The results presented in the table show that CA, LPI, AI, and COH of forest land exhibit significant negative correlations with carbon emissions. In contrast, ENN shows a significant positive correlation with carbon emissions. These findings indicate that larger forest land areas and stronger spatial aggregation and connectivity among forest patches can significantly reduce overall carbon emissions. Conversely, greater fragmentation and dispersion of forest patches weaken the carbon sequestration effect of forest ecosystems.

5. SUMMARY

From 2000 to 2020, total carbon emissions in Ganzhou increased from 9.59 million tons to 36.36 million tons, showing a continuous upward trend over the study period. However, the growth rate gradually slowed after 2010.

The spatial pattern of carbon emissions evolved from a “central-high and peripheral-low” structure in 2000 to a more differentiated pattern characterized by “central > northeast > south > west” in 2020, forming a contiguous high-emission zone centered on Zhanggong and Ruijin. Results from the standard deviational ellipse analysis indicate a gradual northeastward expansion of the carbon emission distribution, accompanied by contraction in other directions. The shortening of the minor axis in 2020 suggests increasing spatial concentration and the emergence of a more pronounced core area.

Carbon emissions exhibited significant positive spatial autocorrelation in 2000, indicating strong clustering characteristics. Over time, the clustering effect weakened, and Moran’s I decreased to 0.102 in 2020, reflecting a more dispersed spatial distribution of emissions. Construction land expansion is significantly positively correlated with carbon emissions, and higher connectivity and aggregation of built-up land patches tend to intensify emissions. In contrast, forest land serves as the primary carbon sink in Ganzhou; larger forest areas and stronger connectivity among forest patches can effectively reduce overall carbon emissions, while fragmentation of forest land weakens its carbon sequestration capacity.

REFERENCES

[1] Lou, Y. (2023). Evolutionary Characteristics of CarbonEmissions in the Central City of Changchunand the design of Community CarbonReduction Units. Jilin Jianzhu University. https://doi.org/10.27714/d.cnki.gjljs.2023.000102

[2] Houghton, J. T. (1996). Revised 1996 IPCC guidelines for national greenhouse gas inventories.

[3] Ouyang, Xiaoling, Lin, & Boqiang. (2017). Carbon dioxide (CO2) emissions during urbanization: A comparative study between China and Japan. Journal of Cleaner Production, 143(FEB.1), 356-368.

[4] Wang, Z., & Pu, C. (2022). Construction and Empirical Evidence of Carbon Emission Accounting System for Urbanization in China. Statistics & Decision, 38(07), 57-61. https://doi.org/10.13546/j.cnki.tiyjc.2022.07.011

[5] Hampf, & Benjamin. (2019). Estimating Emission Coefficients and Mass Balances using Economic Data: A Stochastic Frontier Approach. Journal of Industrial Ecology, 23.

[6] Niu, Y., Zhao, X., & Hu, Y. (2021). Spatial variation of carbon emissions from county land use in Chang-Zhu-Tan area based on NPP-VIIRS night light. Acta Scientiae Circumstantiae, 41(09), 3847-3856. https://doi.org/10.13671/j.hjkoxb.2021.0281

[7] Yu, B., Yang, X., & Wu, X. (2020). Study on spatial spillover effects and influencing factors of carbon emissions in county areas of Ha-Chang city group: Evidence from NPP-VIIRS nightlight data. Acta Scientiae Circumstantiae, 40(02), 697-706.

[8] Raupach, Michael, R., Marland, Gregg, Ciais,…America, C. J. P. o. t. N. A. o. S. o. t. U. S. o. (2007). Global and regional drivers of accelerating CO₂ emissions. Proceedings of the National Academy of Sciences of the United States of America. https://doi.org/10.1073/pnas.0700609104

[9] Zhang, Yan, C., Zhao, Lin, Zhang, Haotian,…Qian. (2022). Spatial-temporal characteristics of carbon emissions from land use change in Yellow River Delta region, China. 136, 108623-.

[10] Chen, Jiandong, Gao, Ming, Cheng, Shulei,…Yuli. (2020). County-level CO2 emissions and sequestration in China during 1997–2017. Scientific Data, 7(7). https://doi.org/10.1038/s41597-020-00736-3

[11] Shi, Yusheng, Matsunaga, Tsuneo, Yamaguchi, Yasushi,…Zhengqiang. (2018). Long-term trends and spatial patterns of PM2.5-induced premature mortality in South and Southeast Asia from 1999 to 2014. Science of The Total Environment.

[12] Huang, H., Jia, J., & Zhang, Z. (2023). Spatiotemporal pattern evolution and influencing factors of land-use carbon emissions in counties, Jiangxi Province. Acta Ecologica Sinica, 43(20), 8390-8403. https://doi.org/10.20103/j.stb.202211293454